Received: 13 December 2020 | Accepted: 1 January 2021

DOI: 10.1111/ene.14717

european journal of neurology
the official journal of the european academy of neurology

ORIGINAL ARTICLE

Structural and functional underpinnings of precentral abnormalities in amyotrophic lateral sclerosis

Luqi Cheng[1] | Yumin Yuan[2] | Xie Tang[1] | Yuan Zhou[3,4] | Chunxia Luo[5] | Daihong Liu[6] | Yuanchao Zhang[1] | Jiuquan Zhang[6]

[1]Key Laboratory for Neuroinformation of the Ministry of Education, School of Life Science and Technology, University of Electronic Science and Technology of China, Chengdu, China

[2]School of Intelligent Technology and Engineering, Chongqing University of Science and Technology, Chongqing, China

[3]CAS Key Laboratory of Behavioral Science, Institute of Psychology, Beijing, China

[4]Department of Psychology, University of Chinese Academy of Sciences, Beijing, China

[5]Department of Neurology, First Affiliated Hospital, Third Military Medical University, Chongqing, China

[6]Department of Radiology, Chongqing University Cancer Hospital, Chongqing Cancer Institute, and Chongqing Cancer Hospital, Chongqing, China

Correspondence
Yuanchao Zhang, School of Life Science and Technology, University of Electronic Science and Technology of China, Chengdu 610054, China.
Jiuquan Zhang, Department of Radiology, Chongqing University Cancer Hospital & Chongqing Cancer Institute & Chongqing Cancer Hospital, Chongqing 400030, China.
Email: yuanchao.zhang8@gmail.com (Y.Z.); zhangjq_radiol@foxmail.com (J.Z.)

Funding information
This study was supported by grants from the National Natural Science Foundation of China (Grant No. 82071883), the combination projects in medicine and engineering of the Fundamental Research Funds of the Central Universities in 2019 (project number 2019CDYGYB008), the Chongqing Key Medical Research Project of Combination of Science and Medicine (grant number 2019ZDXM007), and the 2019 SKY Imaging Research Fund of the Chinese International Medical Foundation (project number Z-2014-07-1912-10).

Abstract

Background and purpose: Amyotrophic lateral sclerosis (ALS) is a progressive neurodegenerative disorder characterized by the loss of both upper and lower motor neurons. Studies using various magnetic resonance imaging (MRI) analytical approaches have consistently identified significant precentral abnormalities in ALS, whereas their structural and functional underpinnings remain poorly understood.

Methods: Using cortical thickness, fractional anisotropy (FA), and effective connectivity, we performed a multimodal MRI study to examine the structural and functional alterations associated with precentral abnormalities in patients with ALS (n = 60) compared with healthy controls (n = 60).

Results: Cortical thickness analysis revealed significant cortical thinning in the right precentral gyrus (PCG), superior frontal gyrus, and superior temporal gyrus in patients with ALS. Tractwise white matter microstructure analyses revealed decreased FA in the tracts connected to the PCG cluster in patients with ALS involving the right corticospinal tract and the middle posterior body of the corpus callosum. Additionally, the cortical thickness of the PCG cluster was found to be positively correlated with FA of the tracts connected to the PCG cluster, suggesting that these two structural features are tightly coupled. Using spectral dynamic causal modelling, effective connectivity analysis among the three regions with cortical thinning revealed decreased self-inhibitory influence in the PCG cluster in patients with ALS, which might be an endophenotypic manifestation of an imbalance in inhibitory and excitatory neurotransmitters in this region.

Conclusions: The present data shed new light on the structural and functional underpinnings of precentral abnormalities in ALS.

Abbreviations: ALS, amyotrophic lateral sclerosis; ALSFRS-R, Revised Amyotrophic Lateral Sclerosis Functional Rating Scale; CC, corpus callosum; CST, corticospinal tract; DCM, dynamic causal modelling; DTI, diffusion tensor imaging; FA, fractional anisotropy; fMRI, functional magnetic resonance imaging; FOV, field of view; FSL, Functional Magnetic Resonance Imaging of the Brain Software Library; $GABA_A$, γ-aminobutyric acid type A; GLM, general linear model; GM, gray matter; HC, healthy controls; MNI, Montreal Neurological Institute; PCG, precentral gyrus; PEB, parametric empirical Bayes; SFG, superior frontal gyrus; STG, superior temporal gyrus; TE, echo time; TMS, transcranial magnetic stimulation; TR, repetition time; VBM, voxel-based morphometry; WM, white matter.

KEYWORDS
amyotrophic lateral sclerosis, cortical thickness, effective connectivity, precentral gyrus, spectral dynamic causal modelling

INTRODUCTION

Amyotrophic lateral sclerosis (ALS) is a progressive neurodegenerative disorder characterized by the degeneration and loss of both upper and lower motor neurons [1] Neuroimaging studies have consistently documented focal structural and functional abnormalities in the primary motor cortex in patients with ALS. For example, voxel-based morphometry (VBM) studies have revealed decreased grey matter (GM) volume in the primary motor cortex in patients with ALS [2,3] and surface-based morphometry studies have found significant cortical thinning in the primary motor cortex in patients with ALS compared with healthy controls (HC) [4,5] Using task-based functional magnetic resonance imaging (fMRI), studies have revealed both decreased and increased cortical activation in the primary motor cortex in patients with ALS compared with HC [6,7] Using resting-state fMRI, studies have reported decreased regional homogeneity and degree centrality in the primary motor cortex [8,9] However, the structural and functional underpinnings of the abnormalities in the primary motor cortex remain obscure.

Using diffusion tensor imaging (DTI), several tract-based spatial statistics analyses have shown a consistent decrease in fractional anisotropy (FA) in the corticospinal tract (CST) and the corpus callosum (CC) [10,11] whereas their relationships with precentral abnormalities remain unknown. Using resting-state functional connectivity, some studies have demonstrated reduced motor network (primary and supplementary motor cortices) connectivity in patients with ALS [12,13] provided little information about the causal interactions within the motor network [14] Simultaneous examinations of white matter (WM) alterations and the causal influences relevant to precentral abnormalities may shed new light on the pathophysiology of ALS.

Here, we performed a multimodal MRI study to investigate the structural and functional brain alterations in a large cohort of patients with ALS compared with demographically matched HC. First, surface-based morphometry was conducted to examine the cortical thickness alterations in patients with ALS (n = 60) compared with HC (n = 60). Second, to examine whether cortical thickness alterations are associated with altered WM microstructure, we extracted the WM tracts interconnecting each pair of regions with cortical thickness alterations and all WM tracts connected to each individual region with cortical thickness alterations and then compared the FA between the two groups. Third, to examine the causal interactions among regions with cortical thickness alterations, the effective connectivity among regions with cortical thickness alterations was estimated using spectral dynamic causal modelling (DCM) and compared between the two groups using the recently proposed parametric empirical Bayes (PEB) algorithm [15]

METHODS

Subjects

A total of 120 subjects (60 patients with ALS and 60 HC) were included in this study. These subjects had also participated in our previous neuroimaging studies [16,17] Briefly, all patients with ALS were enrolled and had been diagnosed with sporadic probable or definite ALS according to the El Escorial criteria. The disease severity of all patients was assessed with the Revised Amyotrophic Lateral Sclerosis Functional Rating Scale (ALSFRS-R), with lower scores indicating greater disability [18] Patients with a family history of motor neuron diseases, a clinical diagnosis of frontotemporal dementia, cognitive impairment (Montreal Cognitive Assessment score < 26), and other major systemic, psychiatric, and neurological illnesses were excluded. The gender- and age-matched HC were recruited from the local community and reported no previous history of neurological or psychiatric conditions. All participants were right-handed. The detailed demographic and clinical characteristics of all participants are shown in Table 1. The study was approved by the Medical Research Ethics Committee of Southwest Hospital, and all subjects gave their written informed consent according to the Helsinki Declaration.

TABLE 1 Demographic and clinical characteristics of the subjects

	ALS, n = 60	HC, n = 60	p
Mean age, years (range)	48.77 (26–69)	48.15 (24–70)	0.73
Gender, male/female	39/21	39/21	1.00
Mean ALSFRS-R (range)	32.62 (16–45)	–	–
Limb/bulbar/both onset	47/12/1	–	–
Classic/LMN-D/ UMN-D/PLS/PMA	43/7/7/2/1	–	–
MoCA score (range)	27.38 (26–30)	27.63(26–30)	0.29
Mean disease duration, months (range)	21.05 (2–132)	–	–
Mean disease progression rate (range)	1.36 (0.02–6.50)	–	–

Note: ALS patients were subdivided into five phenotypes: classic, lower motor neuron dominant (LMN-D), upper motor neuron dominant (UMN-D), primary lateral sclerosis (PLS), and progressive muscular atrophy (PMA).

Abbreviations: ALS, amyotrophic lateral sclerosis; ALSFRS-R, Revised Amyotrophic Lateral Sclerosis Functional Rating Scale; HC, health controls; MoCA, Montreal Cognitive Assessment.

MRI acquisition

All magnetic resonance data, including T1-weighted, diffusion-weighted, and resting-state fMRI images, were acquired for each subject using a Siemens 3T Tim Trio scanner with an eight-channel head coil. Briefly, the high-resolution T1-weighted images were collected using a three-dimensional magnetization-prepared rapid gradient-echo imaging sequence with 176 contiguous sagittal slices (repetition time [TR] = 1900 ms, echo time [TE] = 2.52 ms, inversion time = 900 ms, flip angle = 9°, matrix = 256 × 256, voxel size = 1 × 1×1 mm^3, no gap). DTI data, including collection of a non-diffusion-weighted (b = 0 s/mm^2) image and 64 diffusion-weighted (b = 1000 s/mm^2) images, were acquired using a single-shot twice-refocused spin echo sequence (TR = 10,000 ms, TE = 92 ms, matrix = 128 × 124, field of view [FOV] = 256 × 248 mm^2, thickness 2 mm, 75 axial slices with no slice gap). The resting-state fMRI images were collected using an echo planar imaging sequence (TR = 2000 ms, TE = 30 ms, flip angle = 90°, FOV = 192 × 192 mm^2, matrix = 64 × 64, 36 axial slices, gap = 1 mm, voxel size = 3 × 3×3 mm^3, 240 total volumes). During the resting-state fMRI scans, the subjects were instructed to keep their eyes closed and move as little as possible.

Cortical thickness analysis

Each T1-weighted MRI scan was processed using FreeSurfer (https://surfer.nmr.mgh.harvard.edu/) to obtain a three-dimensional model of the cortical surfaces for cortical thickness measurement. Briefly, the T1-weighted images from the MRI scan were segmented to approximate the voxel-based GM/WM boundary, which was tessellated to produce a triangle-based GM/WM boundary surface. The resulting triangle-based GM/WM surface was then subject to an automatic topological correction procedure to obtain a topologically correct GM/WM surface, which hereafter is referred to as the white surface. Subsequently, the white surface was deformed outward using a deformable surface algorithm to reconstruct the pial surface. The cortical thickness map of each participant was then obtained by using the T-average algorithm. Prior to statistical analysis, the individual cortical thickness maps were resampled onto the standard space and further smoothed with a heat kernel of 20-mm width.

Vertexwise contrasts of cortical thickness maps were performed between HC and patients with ALS using the SurfStat package. Specifically, each contrast was entered into a vertexwise general linear model (GLM) with group, sex, and age as covariates. The results were initially thresholded at a vertexwise $p < 0.001$ and then corrected for multiple comparisons at the cluster level using random field theory. The significance level for clusters was set at a clusterwise $p < 0.05$.

Tractwise WM microstructure analysis

Diffusion-weighted MRI data were processed using the Functional Magnetic Resonance Imaging of the Brain Software Library (FSL; https://fsl.fmrib.ox.ac.uk/fsl/). Principal preprocessing steps included eddy-current and head motion correction and brain tissue extraction [19] FA maps were generated using the DTIFIT procedure by fitting a diffusion tensor model at each voxel. Voxelwise estimates of the fibre orientation distribution were computed using the BEDPOSTX procedure, allowing two fibre directions at each voxel.

To explore whether cortical thickness alterations were associated with WM abnormalities, we examined the between-group differences in FA of the WM tracts interconnecting each pair of regions with cortical thickness alterations and all tracts connected to each individual region with cortical thickness alterations. More specifically, the significant cortical surface labels from the cortical thickness analysis were converted into 2-mm-thick volumetric masks below the white surface using the "mri_label2vol" command in FreeSurfer. The resultant volumetric masks (in Montreal Neurological Institute [MNI] standard space) were then converted into the diffusion space of each subject through FSL's FNIRT and FLIRT. To extract the tracts interconnecting each pair of cortical regions, probabilistic tractography was run from all voxels in one cortical region to the whole brain by drawing 5,000 streamline samples, whereas the other was set as a waypoint mask to select the streamlines via these two regions. To extract the tracts connected to each individual cortical region, 5000 streamline samples were seeded from all voxels of the cortical region to the whole brain. To eliminate spurious connections, voxels with a streamline count of less than 2 were excluded. The resulting volume of tracts was binarized and transformed to MNI space. A population tractogram was obtained by calculating a probabilistic fibre-tract map and thresholding it at 50% probability. Subsequently, we could calculate the mean FA of the tracts for each subject by transforming the population tractogram back into the individual's diffusion space.

Tractwise group comparison of the mean FA of a specific tract was performed by using a two-sample *t*-test. In addition, Pearson correlation coefficient was calculated to examine the relationship between the mean FA of the WM tracts and the ALSFRS-R scores of the patients with ALS. Using the pooled data of the two groups, intermodal correlation analyses were performed to explore whether the cortical thickness of a significant cortical region was correlated with the FA of the WM tracts connected to the corresponding region.

Spectral DCM analysis

Preprocessing of the resting-state fMRI data was performed using the Data Processing Assistant for Resting-State fMRI Advanced Edition toolbox (http://rfmri.org/DPARSF). Principal preprocessing steps included removal of the first 10 time points, slice timing, head motion correction, realignment, spatial normalization to MNI space, spatial smoothing with a 6-mm full width at half maximum Gaussian kernel, bandpass temporal filtering (0.01–0.08 Hz), and regressing out nuisance signals containing head motion parameters, WM, and cerebrospinal fluid.

To explore the effective connectivity among regions with cortical thickness alterations in patients with ALS, the significant cortical

regions (three cortical regions) obtained from the cortical thickness analysis were identified as key nodes for the spectral DCM analysis. In brief, the significant cortical surface labels were converted into binary volumetric masks (filling in all the cortical GM of the corresponding labels) in MNI space using the "mri_label2vol" command in FreeSurfer. The time series of each mask were extracted using Statistical Parametric Mapping 12 (http://www.fil.ion.ucl.ac.uk/spm) by selecting the first principal component from a principal component analysis that included the time series of all voxels within the mask. A fully connected model that had bidirectional connections between any pair of nodes was specified for each subject, containing a total of nine connectivity parameters, including recurrent self-connections. This model was then estimated and inverted for each subject. Following the guide of group effective connectivity, we use the PEB algorithm to perform a second-level analysis to estimate the group mean and the effect of diagnosis for each connectivity parameter. Specifically, we fitted a second-level GLM for the connectivity parameters with two regressors: the first one modelling the group mean and the second one modelling the group differences. Then, we conducted a model comparison to prune parameters from the full model that do not contribute to the model evidence by automatic search. This automatic search was performed by using a method called Bayesian model reduction [15] Then, the parameters from the best reduced models were averaged (i.e., Bayesian model averaging) to identify the connections best describing the mean group effect and between-group differences. In the framework of the PEB algorithm, the parameters best describing the effects of group mean and group difference are reported in terms of the posterior probability value rather than the *p*-value. In this study, posterior probability values greater than 0.95 were considered significant. We further calculated Pearson correlation coefficient to examine the relationship between the effective connectivity showing between-group differences and ALSFRS-R scores.

RESULTS

Cortical thickness analysis

Compared with HC, patients with ALS showed significant cortical thinning in the right precentral gyrus (PCG), the right superior frontal gyrus (SFG), and the right superior temporal gyrus (STG; Figure 1).

Tractwise WM microstructure analysis

Compared with HC, patients with ALS showed no significant FA alterations in the WM tracts interconnecting each pair of cortical regions with cortical thickness alterations. We then reconstructed the WM tracts connected separately to the three clusters (Figure 2a). Specifically, the PCG-related tracts were shown to involve the CST and the middle posterior body of the CC; the SFG-related tracts were shown to involve the anterior middle body of the CC and anterior thalamic radiation; and the STG-related tracts were shown to involve the middle longitudinal fasciculus. Intergroup comparisons of the mean FA of these tracts showed that, compared with HC, the FA of the PCG-related tracts was significantly decreased in patients with ALS, whereas the FA of SFG- and STG-related tracts was unaltered in these patients (Figure 2b). In the patient group, we observed a significant positive correlation between the mean FA of the PCG-related tracts and ALSFRS-R scores ($p = 0.026$, $r = 0.287$; Figure 3). In addition, exploratory intermodal correlation analyses showed a significant positive correlation between the cortical thickness of the PCG cluster and the mean FA of the PCG-related tracts ($p = 0.012$, $r = 0.229$; Figure 4).

Spectral DCM analysis

Using the PEB algorithm, we identified 64 possible model configurations of a fully connected, three-node network across patients with ALS and HC. The parameters best describing the combined group effect included a directional inhibitory influence from the PCG to the SFG and STG and reciprocal inhibitory influence of the SFG on the STG. In addition, self-inhibitory connections were only found in the PCG (Figure 5a). The between-group comparison revealed decreased self-inhibitory influence in the PCG in patients with ALS compared with HC (Figure 5b). In addition, correlation analysis showed no significant correlation between the self-inhibitory influence of the PCG and ALSFRS-R scores ($r = -0.033$, $p = 0.8$).

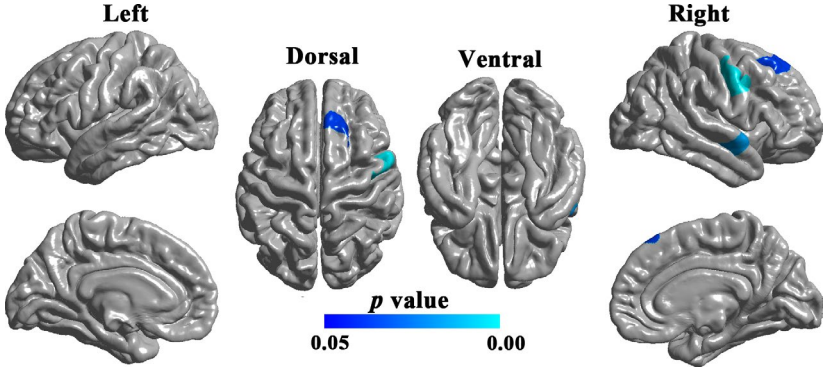

FIGURE 1 Brain regions showing significant cortical thinning in patients with ALS compared with healthy controls. The color bar indicates the corrected *p*-value using random field theory [Colour figure can be viewed at wileyonlinelibrary.com]

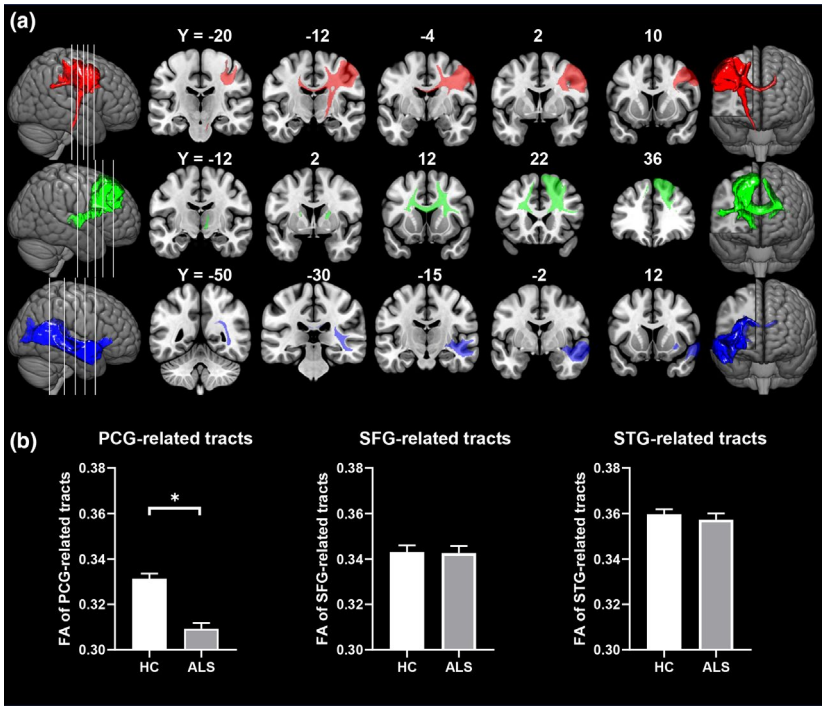

FIGURE 2 Tractwise fractional anisotropy (FA) analysis of the two groups. (a) Three-dimensional and coronal views of the population-based white matter tracts connected respectively to the precentral gyrus (PCG; top), superior frontal gyrus (SFG; middle), and superior temporal gyrus (STG; bottom). (b) Mean FA of the PCG-, SFG-, and STG-related tracts in patients with amyotrophic lateral sclerosis (ALS) and healthy controls (HC). The error bar indicates the standard error of the mean. *Significant between-group difference at the level of $p < 0.001$ [Colour figure can be viewed at wileyonlinelibrary.com]

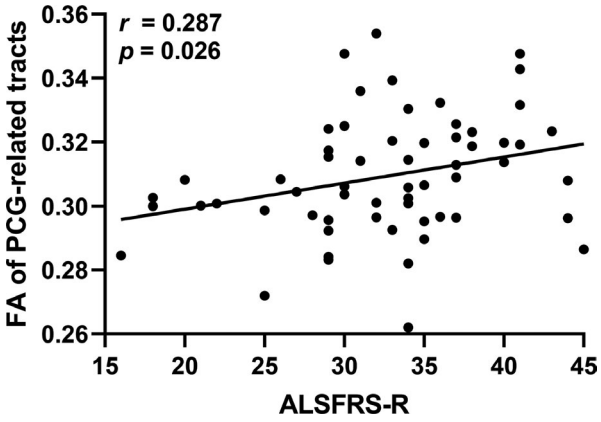

FIGURE 3 Positive correlation between mean fractional anisotropy (FA) of the precentral gyrus (PCG)-related tracts and Revised Amyotrophic Lateral Sclerosis Functional Rating Scale (ALSFRS-R) in patients with amyotrophic lateral sclerosis

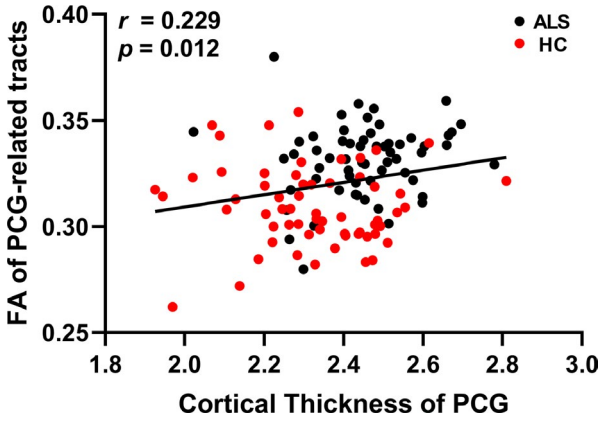

FIGURE 4 Positive correlation between the mean cortical thickness of the precentral gyrus (PCG) cluster and the mean fractional anisotropy (FA) of the PCG-related tracts using data of both groups. ALS, amyotrophic lateral sclerosis; HC, healthy controls [Colour figure can be viewed at wileyonlinelibrary.com]

DISCUSSION

In this study, we performed a multimodal MRI-based analysis to examine the structural and functional alterations in patients with ALS compared with HC. The key findings of this study can be summarized as follows. First, compared with HC, significant cortical thinning was found in patients with ALS, involving the right PCG, right SFG, and right STG. Second, compared with HC, patients with ALS showed decreased FA in the WM tracts connected to the PCG cluster (involving the CST and the middle posterior body of the CC), which was also found to be positively correlated with ASLFRS-R scores. Additionally, the cortical thickness of the PCG cluster was found to be positively correlated with the mean FA of the PCG-related WM tracts. Third, compared with HC, spectral DCM analysis showed decreased self-inhibitory influence in the PCG in patients with ALS. Taken together, these findings shed new light on the structural and functional underpinnings of precentral abnormalities in ALS.

Cortical thinning in ALS

Our finding of cortical thinning in the right PCG in patients with ALS is of particular interest and is in agreement with previous cortical thickness studies of ALS [4,5,20] Moreover, this finding is also

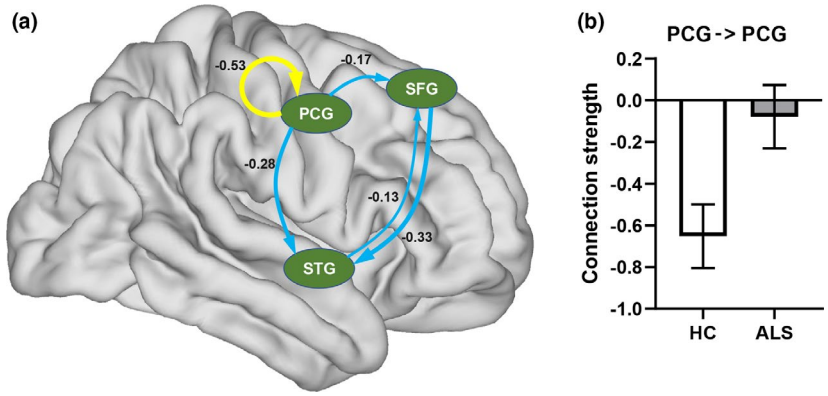

FIGURE 5 Effective connectivity among the precentral gyrus (PCG), superior frontal gyrus (SFG), and superior temporal gyrus (STG). (a) A schematic illustration of the significant effective connectivity among the three nodes. The intrinsic inhibitory self-connection was color-coded in yellow, whereas the extrinsic inhibitory connection was color-coded in blue. (b) Significantly decreased self-connection of the PCG cluster in patients with amyotrophic lateral sclerosis (ALS) compared with healthy controls (HC). Connectivity changes with a posterior probability value > 0.95 were considered significant. The error bar indicates the 95% confidence interval [Colour figure can be viewed at wileyonlinelibrary.com]

supported by previous VBM studies reporting precentral GM atrophy in patients with ALS [2,3] Using susceptibility-weighted imaging, one recent texture analysis study found altered precentral texture feature autocorrelation in patients with ALS [21] Because cortical thickness is thought to reflect the size, density, and arrangement of cells, cortical thickness reductions may indicate the occurrence of substantial changes in the size, number, and/or organization of cells in the overlying brain region. Presumably, the observed cortical thinning in the PCG might be a macroscopic manifestation of the loss of giant Betz cells and the relatively smaller size of the remaining pyramidal cells in Layer V of the PCG in patients with ALS, as previously reported in postmortem studies [22–24] The exact mechanisms underlying precentral thinning, however, remain unknown and need further investigation. Collectively, the observed cortical thinning in the PCG, together with that observed from previous reports [2–5,20] suggests that cortical structural abnormalities in the PCG might be considered a common feature in patients with ALS.

Compared with HC, the present study also showed significant cortical thinning in the right SFG and right STG in patients with ALS. This finding is consistent with previous studies, which reported decreased GM volume and thickness in several brain regions, including the SFG and STG [25,26] Functionally, the SFG, which is located in the dorsolateral prefrontal cortex, has been shown to play a crucial role in working memory [27] and attention [28] The STG has been involved in speech perception [29] and emotion recognition [30] In ALS, a number of studies have reported varying degrees of impairments in the language, cognitive, and behavioural domains, such as frontal executive deficits that involve verbal fluency, attention, and working memory [31,32] and facial or prosodic emotion recognition deficits, especially for disgust and surprise [33,34] The finding of significant cortical thinning in the SFG and STG might be the anatomical substrate underlying such nonmotor impairments in patients with ALS and adds further evidence for a continuum between ALS and frontotemporal dementia.

Abnormal WM microstructure of PCG-related tracts in ALS

Compared with HC, patients with ALS showed decreased FA in the WM tracts connected to the precentral cluster with cortical thinning, involving the right CST and the middle posterior body of the CC. This finding is consistent with previous reports on WM microstructural alterations in ALS [10,11] The CST, approximately 30% of whose neurons originate in the primary motor cortex [35,36] is of particular importance to the motor system, because it mediates voluntary movements of the distal extremities [37] The CC, with its middle posterior body connecting the primary motor cortices of the bilateral hemispheres, also plays an essential role in motor functioning [38,39] Given that in the patient group, the present study demonstrated a positive correlation between ALSFRS-R scores and the mean FA of these tracts, it is therefore tempting to speculate that the observed FA reductions in these tracts may play a role in some of the motor impairments in ALS, such as weak lip sealing, difficulty walking, and loss of hand dexterity [40]

Methodologically, FA measures the directional selectivity of the random diffusion of water molecules along the WM tract [41] and has been considered an indicator of the integrity of the underlying WM tract. FA values are sensitive to several tissue characteristics, such as regional myelination, axonal diameter, axonal density, and axonal organization [42] WM neuropathological alterations, including demyelination, axonal damage, proliferation of glial cells, and intraneuronal abnormalities, have been demonstrated by previous studies [1,43,44] and therefore may account for the observed FA decreases in CST and CC in patients with ALS.

Decreased self-inhibition of the PCG in ALS

Compared with HC, spectral DCM analysis showed decreased self-inhibition in the PCG in patients with ALS, suggestive of disinhibition

(i.e., cortical hyperexcitability) in this region. This result is supported by previous studies reporting reduced expression of γ-aminobutyric acid type A ($GABA_A$) receptors, loss of binding of the $GABA_A$ receptor ligand [11C]-flumazenil, and loss of parvalbumin-positive inhibitory cortical interneurons in the motor cortex in patients with ALS [45–47] Studies using transcranial magnetic stimulation (TMS) have provided corroborating evidence for a disinhibited motor cortex by showing significant decreases in short-interval intracortical inhibition in patients with ALS [48] In parallel, some task-based positron emission tomography and fMRI studies have documented increased cortical activation in the motor cortex during the performance of a motor task [49,50] In addition, TMS studies have also reported significant increases in intracortical facilitation, the amplitude of motor-evoked potentials, and cortical stimulus–response curve gradients, and significant decreases in the resting motor threshold in patients with ALS, all of which are indicative of a hyperexcitable motor cortex [48,51]

Considering that self-inhibition of one node in the DCM was suggested to control the region's excitatory–inhibitory balance [52] the impaired self-inhibition of the PCG therefore suggests that the normal excitatory–inhibitory balance in the PCG is disrupted in patients with ALS. The disruption of the excitatory–inhibitory balance in the PCG may arise as a result of an imbalance in inhibitory and excitatory neurotransmitters in this region. As is known, glutamate and GABA are respectively the principal excitatory and inhibitory neurotransmitters in the central nervous system [53] In previous studies, GABA concentrations were shown to be negatively correlated with stimulus-induced activity within the measured regions [54] whereas glutamate concentrations were found to be negatively correlated with the inhibitory influence on the excitatory cortical areas [54,55] Notably, both elevated levels of Glx (a combined measure of glutamate and glutamine) and reduced levels of GABA have been documented in the motor cortex in patients with ALS [56,57] It is therefore possible that the imbalance in inhibitory and excitatory neurotransmitters, caused by elevated levels of glutamate, reduced levels of GABA, or both, results in a disrupted excitatory–inhibitory balance in the PCG, which manifests endophenotypically as decreased precentral self-inhibition in patients with ALS. Nonetheless, abnormal levels of some monoamine neurotransmitters, such as dopamine, serotonin, and norepinephrine, could also have contributed to the disruption of the excitatory–inhibitory balance in the PCG, as alterations in concentrations of these neurotransmitters have been reported in ALS as well [58–61] This idea was supported by previous studies showing that dopamine signaling and reductions of serotonin activity were associated with increase in functional connectivity and activity in sensory–motor areas [62–64] and that noradrenergic enhancement could improve motor network connectivity in stroke patients [65] However, such an interpretation should be taken with caution, because these monoamine neurotransmitters could be both excitatory and inhibitory, depending on the type of receptor that they bind to [66] Given that the present study found no significant correlation between the self-inhibition of the PCG and clinical symptoms (assessed with ALSFRS-R scores) in patients with ALS, we cannot determine the clinical correlates of the disruption of the excitatory–inhibitory balance in the PCG. Future studies are therefore needed to further pursue this issue.

CONCLUSIONS

Using multimodal MRI data, the present study identified significant decreases in precentral cortical thickness, precentral self-inhibition, and FA of PCG-related WM tracts in patients with ALS compared with HC. These findings shed new light on the structural and functional underpinnings of precentral abnormalities in ALS.

ACKNOWLEDGMENT

We thank all patients and controls for their participation in our study.

CONFLICT OF INTEREST

The authors report no competing interests.

AUTHOR CONTRIBUTION

Luqi Cheng: formal analysis (equal), investigation (equal), methodology (equal), validation (equal), writing–original draft (equal), writing–review & editing (equal). Yumin Yuan: formal analysis (equal), investigation (equal), writing–review & editing (equal). Xie Tang: formal analysis (equal), investigation (equal), writing–review & editing (equal). Yuan Zhou: investigation (equal), writing–review & editing (equal). Chunxia Luo: investigation (equal), writing–review & editing (equal). Daihong Liu: investigation (equal), writing–review & editing (equal). Yuanchao Zhang: conceptualization (equal), data curation (equal), formal analysis (equal), investigation (equal), methodology (equal), project administration (equal), resources (equal), supervision (equal), validation (equal), writing–original draft (equal), writing–review & editing (equal). Jiuquan Zhang: conceptualization (equal), data curation (equal), funding acquisition (equal), resources (equal), validation (equal), writing–review & editing (equal).

DATA AVAILABILITY STATEMENT

The data that support the findings of this study are available from the corresponding author upon reasonable request from a qualified investigator.

ORCID

Yuanchao Zhang https://orcid.org/0000-0001-8191-4899

REFERENCES

1. Turner MR, Agosta F, Bede P, Govind V, Lulé D, Verstraete E. Neuroimaging in amyotrophic lateral sclerosis. *Biomark Med*. 2012;6:319-337.
2. Agosta F, Pagani E, Rocca M, et al. Voxel-based morphometry study of brain volumetry and diffusivity in amyotrophic lateral sclerosis patients with mild disability. *Hum Brain Mapp*. 2007;28:1430-1438.

3. Devine MS, Pannek K, Coulthard A, McCombe PA, Rose SE, Henderson RD. Exposing asymmetric gray matter vulnerability in amyotrophic lateral sclerosis. *Neuroimage Clin*. 2015;7:782-787.
4. Mezzapesa DM, D'Errico E, Tortelli R, et al. Cortical thinning and clinical heterogeneity in amyotrophic lateral sclerosis. *PLoS ONE*. 2013;8:e80748.
5. Walhout R, Westeneng H-J, Verstraete E, et al. Cortical thickness in ALS: towards a marker for upper motor neuron involvement. *J Neurol Neurosurg Psychiatry*. 2015;86:288-294.
6. Schoenfeld MA, Tempelmann C, Gaul C, et al. Functional motor compensation in amyotrophic lateral sclerosis. *J Neurol*. 2005;252:944-952.
7. Stoppel CM, Vielhaber S, Eckart C, et al. Structural and functional hallmarks of amyotrophic lateral sclerosis progression in motor-and memory-related brain regions. *Neuroimage Clin*. 2014;5:277-290.
8. Zhou F, Xu R, Dowd E, Zang Y, Gong H, Wang Z. Alterations in regional functional coherence within the sensory-motor network in amyotrophic lateral sclerosis. *Neurosci Lett*. 2014;558:192-196.
9. Zhou C, Hu X, Hu J, et al. Altered brain network in amyotrophic lateral sclerosis: a resting graph theory-based network study at voxel-wise level. *Front Neurosci*. 2016;10:204.
10. Filippini N, Douaud G, Mackay C, Knight S, Talbot K, Turner M. Corpus callosum involvement is a consistent feature of amyotrophic lateral sclerosis. *Neurology*. 2010;75:1645-1652.
11. Douaud G, Filippini N, Knight S, Talbot K, Turner MR. Integration of structural and functional magnetic resonance imaging in amyotrophic lateral sclerosis. *Brain*. 2011;134:3470-3479.
12. Jelsone-Swain LM, Fling BW, Seidler RD, Hovatter R, Gruis K, Welsh RC. Reduced interhemispheric functional connectivity in the motor cortex during rest in limb-onset amyotrophic lateral sclerosis. *Front Syst Neurosci*. 2010;4:158.
13. Tedeschi G, Trojsi F, Tessitore A, et al. Interaction between aging and neurodegeneration in amyotrophic lateral sclerosis. *Neurobiol Aging*. 2012;33:886-898.
14. Friston KJ, Harrison L, Penny W. Dynamic causal modelling. *NeuroImage*. 2003;19:1273-1302.
15. Friston KJ, Litvak V, Oswal A, et al. Bayesian model reduction and empirical Bayes for group (DCM) studies. *NeuroImage*. 2016;128:413-431.
16. Zhang Y, Qiu T, Yuan X, et al. Abnormal topological organization of structural covariance networks in amyotrophic lateral sclerosis. *Neuroimage Clin*. 2019;21:101619.
17. Qiu T, Zhang Y, Tang X, et al. Precentral degeneration and cerebellar compensation in amyotrophic lateral sclerosis: a multimodal MRI analysis. *Hum Brain Mapp*. 2019;40:3464-3474.
18. Cedarbaum JM, Stambler N, Malta E, et al. The ALSFRS-R: a revised ALS functional rating scale that incorporates assessments of respiratory function. *J Neurol Sci*. 1999;169:13-21.
19. Smith SM. Fast robust automated brain extraction. *Hum Brain Mapp*. 2002;17:143-155.
20. Contarino VE, Conte G, Morelli C, et al. Toward a marker of upper motor neuron impairment in amyotrophic lateral sclerosis: a fully automatic investigation of the magnetic susceptibility in the precentral cortex. *Eur J Radiol*. 2020;124:108815.
21. Johns SL, Ishaque A, Khan M, Yang Y-H, Wilman AH, Kalra S. Quantifying changes on susceptibility weighted images in amyotrophic lateral sclerosis using MRI texture analysis. *Amyotroph Lat Scl Fr*. 2019;20:1-8.
22. Saberi S, Stauffer JE, Schulte DJ, Ravits J. Neuropathology of amyotrophic lateral sclerosis and its variants. *Neurol Clin*. 2015;33:855-876.
23. Riku Y, Atsuta N, Yoshida M, et al. Differential motor neuron involvement in progressive muscular atrophy: a comparative study with amyotrophic lateral sclerosis. *BMJ open*. 2014;4.e005213
24. Genç B, Jara JH, Lagrimas AK, et al. Apical dendrite degeneration, a novel cellular pathology for Betz cells in ALS. *Sci Rep*. 2017;7:41765.
25. Chang J, Lomen-Hoerth C, Murphy J, et al. A voxel-based morphometry study of patterns of brain atrophy in ALS and ALS/FTLD. *Neurology*. 2005;65:75-80.
26. Agosta F, Valsasina P, Riva N, et al. The cortical signature of amyotrophic lateral sclerosis. *PLoS ONE*. 2012;7:e42816.
27. Owen AM, Stern CE, Look RB, Tracey I, Rosen BR, Petrides M. Functional organization of spatial and nonspatial working memory processing within the human lateral frontal cortex. *Proc Natl Acad Sci USA*. 1998;95:7721-7726.
28. Corbetta M, Patel G, Shulman GL. The reorienting system of the human brain: from environment to theory of mind. *Neuron*. 2008;58:306-324.
29. Jäncke L, Wüstenberg T, Scheich H, Heinze H-J. Phonetic perception and the temporal cortex. *NeuroImage*. 2002;15:733-746.
30. Hoekert M, Bais L, Kahn RS, Aleman A. Time course of the involvement of the right anterior superior temporal gyrus and the right fronto-parietal operculum in emotional prosody perception. *PLoS ONE*. 2008;3:e2244.
31. Abrahams S, Goldstein L, Simmons A, et al. Word retrieval in amyotrophic lateral sclerosis: a functional magnetic resonance imaging study. *Brain*. 2004;127:1507-1517.
32. Phukan J, Pender NP, Hardiman O. Cognitive impairment in amyotrophic lateral sclerosis. *Lancet Neurol*. 2007;6:994-1003.
33. Benbrika S, Desgranges B, Eustache F, Viader F. Cognitive, emotional and psychological manifestations in amyotrophic lateral sclerosis at baseline and overtime: a review. *Front Neurosci*. 2019;13:951.
34. Martins AP, Prado LdGR, Lillo P, Mioshi E, Teixeira AL, De Souza LC. Deficits in emotion recognition as markers of frontal behavioral dysfunction in amyotrophic lateral sclerosis. *J Neuropsychiatry Clin Neurosci*. 2019;31:165-169.
35. Seo J, Jang S. Different characteristics of the corticospinal tract according to the cerebral origin: DTI study. *AJNR Am J Neuroradiol*. 2013;34:1359-1363.
36. Standring S. *Gray's anatomy: the anatomical basis of clinical practice*, Elsevier Health Sciences; 2015.
37. Welniarz Q, Dusart I, Roze E. The corticospinal tract: evolution, development, and human disorders. *Dev Neurobiol*. 2017;77:810-829.
38. Wahl M, Lauterbach-Soon B, Hattingen E, et al. Human motor corpus callosum: topography, somatotopy, and link between microstructure and function. *J Neurosci*. 2007;27:12132-12138.
39. Zhang J, Ji B, Hu J, et al. Aberrant interhemispheric homotopic functional and structural connectivity in amyotrophic lateral sclerosis. *J Neurol Neurosurg Psychiatry*. 2017;88:369-370.
40. Gordon PH. Amyotrophic lateral sclerosis: an update for 2013 clinical features, pathophysiology, management and therapeutic trials. *Aging Dis*. 2013;4:295.
41. Basser PJ. Focal magnetic stimulation of an axon. *IEEE Trans Biomed Eng*. 1994;41:601-606.
42. Beaulieu C. The basis of anisotropic water diffusion in the nervous system–a technical review. *NMR Biomed*. 2002;15:435-455.
43. Kang SH, Li Y, Fukaya M, et al. Degeneration and impaired regeneration of gray matter oligodendrocytes in amyotrophic lateral sclerosis. *Nat Neurosci*. 2013;16:571-579.
44. Ferraiuolo L, Meyer K, Sherwood TW, et al. Oligodendrocytes contribute to motor neuron death in ALS via SOD1-dependent mechanism. *Proc Natl Acad Sci USA*. 2016;113:E6496-E6505.
45. Nihei K, McKee AC, Kowall NW. Patterns of neuronal degeneration in the motor cortex of amyotrophic lateral sclerosis patients. *Acta Neuropathol*. 1993;86:55-64.
46. Lloyd C, Richardson M, Brooks D, Al-Chalabi A, Leigh P. Extramotor involvement in ALS: PET studies with the GABAA ligand [11C] flumazenil. *Brain*. 2000;123:2289-2296.
47. Petri S, Krampfl K, Hashemi F, et al. Distribution of GABAA receptor mRNA in the motor cortex of ALS patients. *J Neuropathol Exp Neurol*. 2003;62:1041-1051.

48. Vucic S, Cheah BC, Kiernan MC. Defining the mechanisms that underlie cortical hyperexcitability in amyotrophic lateral sclerosis. *Exp Neurol*. 2009;220:177-182.
49. Kew J, Leigh P, Playford E, et al. Cortical function in amyotrophic lateral sclerosis: a positron emission tomography study. *Brain*. 1993;116:655-680.
50. Kollewe K, Münte TF, Samii A, Dengler R, Petri S, Mohammadi B. Patterns of cortical activity differ in ALS patients with limb and/or bulbar involvement depending on motor tasks. *J Neurol*. 2011;258:804-810.
51. Williams KL, Fifita JA, Vucic S, et al. Pathophysiological insights into ALS with C9ORF72 expansions. *J Neurol Neurosurg Psychiatry*. 2013;84:931-935.
52. Bastos AM, Usrey WM, Adams RA, Mangun GR, Fries P, Friston KJ. Canonical microcircuits for predictive coding. *Neuron*. 2012;76:695-711.
53. Petroff OA. Book review: GABA and glutamate in the human brain. *Neuroscientist*. 2002;8:562-573.
54. Duncan NW, Wiebking C, Northoff G. Associations of regional GABA and glutamate with intrinsic and extrinsic neural activity in humans—a review of multimodal imaging studies. *Neurosci Biobehav Rev*. 2014;47:36-52.
55. Limongi R, Jeon P, Mackinley M, et al. Glutamate and Dysconnection in the salience network: Neurochemical, effective-connectivity, and computational evidence in schizophrenia. *Biol Psychiatry*. 2020;88:273–281.
56. Foerster B, Callaghan B, Petrou M, Edden RAE, Chenevert T, Feldman E. Decreased motor cortex γ-aminobutyric acid in amyotrophic lateral sclerosis. *Neurology*. 2012;78:1596-1600.
57. Foerster BR, Pomper MG, Callaghan BC, et al. An imbalance between excitatory and inhibitory neurotransmitters in amyotrophic lateral sclerosis revealed by use of 3-T proton magnetic resonance spectroscopy. *JAMA Neurol*. 2013;70:1009-1016.
58. Bertel O, Malessa S, Sluga E, Hornykiewicz O. Amyotrophic lateral sclerosis: changes of noradrenergic and serotonergic transmitter systems in the spinal cord. *Brain Res*. 1991;566:54-60.
59. Turner M, Rabiner E, Al-Chalabi A, et al. Cortical 5-HT1A receptor binding in patients with homozygous D90A SOD1 vs sporadic ALS. *Neurology*. 2007;68:1233-1235.
60. Fu X, Zhu W, Guo Z, et al. 18F-fallypride PET-CT of dopamine D2/D3 receptors in patients with sporadic amyotrophic lateral sclerosis. *J Neurol Sci*. 2017;377:79-84.
61. Vermeiren Y, Janssens J, Van Dam D, De Deyn PP. Serotonergic dysfunction in amyotrophic lateral sclerosis and Parkinson's disease: similar mechanisms, dissimilar outcomes. *Front Neurosci*. 2018;12:185.
62. Kunisato Y, Okamoto Y, Okada G, et al. Modulation of default-mode network activity by acute tryptophan depletion is associated with mood change: a resting state functional magnetic resonance imaging study. *Neurosci Res*. 2011;69:129-134.
63. Alavash M, Lim S-J, Thiel C, Sehm B, Deserno L, Obleser J. Dopaminergic modulation of hemodynamic signal variability and the functional connectome during cognitive performance. *NeuroImage*. 2018;172:341-356.
64. Conio B, Martino M, Magioncalda P, et al. Opposite effects of dopamine and serotonin on resting-state networks: review and implications for psychiatric disorders. *Mol Psychiatry*. 2020;25:82-93.
65. Wang LE, Fink GR, Diekhoff S, Rehme AK, Eickhoff SB, Grefkes C. Noradrenergic enhancement improves motor network connectivity in stroke patients. *Ann Neurol*. 2011;69:375-388.
66. Rubenstein J, Merzenich MM. Model of autism: increased ratio of excitation/inhibition in key neural systems. *Genes Brain Behav*. 2003;2:255-267.

How to cite this article: Cheng L, Yuan Y, Tang X, et al. Structural and functional underpinnings of precentral abnormalities in amyotrophic lateral sclerosis. *Eur J Neurol*. 2021;28:1528–1536. https://doi.org/10.1111/ene.14717